ELSEVIER

Contents lists available at ScienceDirect

### **Electric Power Systems Research**

journal homepage: www.elsevier.com/locate/epsr





## Fast frequency regulation of virtual power plants via Droop Reset Integral Control (DRIC)<sup>☆</sup>

Vishal Shenoy <sup>a</sup>, Paul Serna-Torre <sup>b,c</sup>, David Schoenwald <sup>d</sup>, Patricia Hidalgo-Gonzalez <sup>a,b,c</sup>, Jorge I. Poveda <sup>a,\*</sup>

- <sup>a</sup> Department of Electrical and Computer Engineering, University of California, San Diego, United States
- <sup>b</sup> Department of Mechanical and Aerospace Engineering, University of California, San Diego, United States
- <sup>c</sup> Center for Energy Research, University of California, San Diego, United States
- <sup>d</sup> Sandia National Laboratories, Albuquerque, NM 87185, USA

#### ARTICLE INFO

# Keywords: Ancillary services Frequency control Hybrid control Reset control Virtual power plant

#### ABSTRACT

We consider the frequency regulation problem for a Virtual Power Plant (VPP) consisting of inverter-interfaced distributed energy resources connected to a power grid, modeled macroscopically, by a conventional generator connected to multiple time-varying loads. To improve the transient performance (settling time, overshoot, etc.) of the frequency response under load disturbances, we introduce a novel Droop Reset Integral Control (DRIC) law that synergistically combines resetting integrators with integral droop controllers (also referred to as proportional integral (PI) control in the literature). We prove the stability of the proposed control scheme, and its robustness to external disturbances, using conditions based on linear matrix inequalities (LMI) that can be numerically verified a priori. Furthermore, we validate the proposed approach using both learned voltage source inverter dynamics and a high-fidelity Simscape model developed by Sandia National Laboratories. Our results show that the DRIC algorithm is able to significantly reduce overshoot, induce zero steady-state error, and decrease settling times up to 7 times that of standard droop and PI control. We also provide heuristic tuning guidelines for the proposed controller, which can be particularly useful for system operators whenever a detailed model of the virtual power plant is unavailable.

#### 1. Introduction

Due to the volatile nature of the current global climate conditions, there has been a steady rise in the adoption of distributed energy resources (DERs) accompanied by a simultaneous departure from the use of fossil fuel technologies. As a side effect, the modern power grid continues to experience a decline in system inertia [1], a mechanism that aids in the stability of power grids dominated by synchronous machines. With reduced margins of stability and robustness, there is a need to effectively coordinate the available DERs and to provide ancillary services to the grid [2]. A potential solution to this multi-agent coordination problem is the development and incorporation of the so called Virtual Power Plants (VPPs), first introduced in [3]. VPPs can be envisioned as distributed power plants primarily operating in a gridtied mode. They synergistically coordinate a collection of DERs (not necessarily co-located) to emulate the behavior of a traditional power

plant. For a detailed survey of the various components of VPPs and related feedback control schemes from a multi-agent, cyber–physical systems perspective, we refer the reader to the recent survey paper [4].

In this work, we address the frequency regulation problem of VPPs. Traditionally, frequency regulation is addressed using droop control, as discussed in [5]. In [6], the authors utilized a synthetic inertia based approach within a cluster of inverter-based resources to provide frequency regulation, compensating for the loss of synchronous inertial response from conventional generators. In [7] a dynamic variant of the classical droop control was introduced to overcome the problem of unbounded noise amplification in controllers with synthetic inertia in the presence of measurement noise. However, these control strategies are susceptible to non-zero steady-state errors due to the lack of integral action. This deficiency can result in a deviation of the grid frequency from the nominal 60 Hz at steady state, as depicted in [8].

E-mail addresses: vshenoy@ucsd.edu (V. Shenoy), psernatorre@ucsd.edu (P. Serna-Torre), daschoe@sandia.gov (D. Schoenwald), phidalgogonzalez@ucsd.edu (P. Hidalgo-Gonzalez), poveda@ucsd.edu (J.I. Poveda).

https://doi.org/10.1016/j.epsr.2024.110762

roject supported in part by Sandia National Laboratories, United States under the project Clusters of Flexible PV-Wind-Storage Hybrid Generation (FlexPower), and by the NSF Grant CAREER: ECCS 2305756. P.S. is partially supported a scholarship from the Peru Ministry of Education.

<sup>\*</sup> Corresponding author.

A natural solution to this problem is to augment the standard droop controller with integral action, as demonstrated in [5], leading to a PI (proportional plus integral) feedback structure. In [9], the authors employed a variant of the droop controller by dynamically updating the controller gains. While this approach has been shown to improve transient and steady-state performance compared to their static counterparts, it can suffer from robustness issues in the presence of noisy measurements. It is important to note that even though PI controllers can result in zero steady-state error, standard linear controllers are bound by fundamental limitations, as shown in [10], which cannot be overcome without incorporating non-linear or non-smooth control mechanisms.

On the other hand, nonlinear controllers, such as sliding mode control (SMC) [11] and model predictive control (MPC) [12], have also found applications in frequency regulation of power systems. However, SMC suffers from the chattering phenomenon occurring along the sliding surface, and MPC, while guaranteeing optimality, incurs high computational costs which could be detrimental as the scale of the VPP grows. Therefore, there is a pressing need for developing nonlinear controllers capable of overcoming fundamental limitations of linear controllers while simultaneously remaining computationally feasible and robust to noise. In this context, reset-based controllers emerge as a promising option.

The concept of using resetting integrators in dynamical systems to improve transient performance was introduced by Clegg in [13]. The Clegg integrator is a linear integrator that resets its output to zero when the signs of its input and output differ. The advantages of this component can be quantified through its describing function, which exhibits the same magnitude plot as a regular integrator but with a 51.9° smaller phase lag than its linear counterpart. Clegg further showed that such a resetting mechanism could systematically address fundamental limitations faced by linear controllers. However, it was not until the work presented in [14] that a concrete example of an integrator plant overcoming overshoot and rise time constraints, which could not be satisfied by a standard linear controller, was demonstrated. A necessary and sufficient condition for stability based on the strict positive realness of transfer matrices was later established in [15]. For a survey of early stability results on reset control, we direct the reader to [16].

The modern approach to modeling reset controllers leverages tools from hybrid dynamical systems. First proposed in [17], the first-order reset element (FORE) introduced an additional tuning parameter for adjusting the overshoot response while reducing to the standard Clegg integrator when the parameter is set to zero. Furthermore, the FORE constitutes a well-posed hybrid system, as defined in [18], which offers several theoretical guarantees in terms of existence of solutions, stability and robustness to measurement noise. A comprehensive treatment of the stability properties of FOREs can be found in [19].

In the context of frequency regulation, reset controllers were studied in [20] to perform load frequency control of an islanded microgrid. However, this approach considered fixed pre-scheduled reset times rather than state-based resets. In turn, fixed reset times require optimal tuning of the reset frequency to induce a suitable transient performance. Such optimal tuning is difficult to obtain whenever the underlying dynamics of the system are unknown, as demonstrated in [19]. In [21], the authors also considered the frequency regulation problem of an islanded microgrid in the presence of parametric uncertainty. However, no theoretical guarantees on closed-loop stability and robustness were provided. Indeed, to the best of our knowledge, no previous work has addressed the frequency regulation problem of VPPs using state-based reset laws while simultaneously providing stability and robustness guarantees.

In this work, we propose an extension of the familiar droop-based controllers and their variants by incorporating nonlinear resetting integrators [22] to enhance transient performance and overcome the fundamental limitations faced by smooth linear controllers, as demonstrated in [14]. Additionally, we provide theoretical guarantees for the

proposed controller by leveraging tools from hybrid control theory. Moreover, we validate our approach on a high-fidelity model that demonstrates significant improvements in overshoot and settling time compared to standard controllers such as droop control and its variants.

#### 2. Statement of contributions

The following are the main contributions of this work:

- (1) First, and motivated by the fundamental limitations of existing linear and smooth frequency controllers in terms of transient performance, we introduce a novel reset-based controller for frequency regulation in power systems. The proposed controller, termed Droop Reset Integral Control (DRIC), can be seen as a standard droop-integral controller extended with an integrator that is reset to zero whenever a suitable condition is satisfied by the frequency error. Such resets can significantly improve the transient performance of the system by removing, or significantly attenuating the overshoot induced by the control system. Since the proposed controller combines continuous-time dynamics (i.e., proportional integral action) and discrete-time dynamics (i.e., integrator resets), we study the stability properties of the closed-loop system and establish an Input-to-State Stability result using tools from hybrid dynamical systems theory [18].
- (2) To validate the performance of the proposed controller, we test the algorithm in the high-fidelity non-linear FlexPower model [6,23], developed by Sandia National Laboratories, which models a VPP that incorporates wind turbines (WT), photovoltaic cell systems (PVs), battery energy storage systems (BESS), and dynamic loads. The numerical results showed that DRIC can yield significant improvements in terms of transient response in VPPs when compared to conventional linear and smooth controllers, such as droop control, its dynamic variants, and droop integral control.
- (3) We further test the performance of the proposed algorithm with respect to external disturbances acting on the power system. We show that the DRIC method is able to recover the nominal, steady-state frequency of the VPP from sudden load changes in the grid, without requiring parameter re-tuning of the controllers. This inherent "adaptability" feature, inherent to integral action, holds significant practical value for real-world applications.
- (4) Finally, we provide heuristic guidelines for the initial tuning of the DRIC before it is subjected to multiple time-varying load disturbances. These guidelines are particularly useful for system operators in the absence of a detailed VPP model. Typical values of the nominal reset gain are given. Parameters that affect the influence of reset actions when the frequency response is far away from the steady-state are stated. Additionally, the effect of the reset gain parameter on the trade-off between overshoot and settling time is highlighted.

The rest of the paper is organized as follows: In Section 3 we introduce some mathematical preliminaries on hybrid control systems that combine continuous-time and discrete-time dynamics (complemented in the Appendix). Section 4 formulates the frequency regulation problem, explains the setup considered in the paper, and provides a brief overview of our proposed controller. In Section 5, we describe the dynamics of the individual DERs and the proposed controller, verify sufficient conditions for closed-loop stability, and robustness and apply said results on a learnt linearized model of a VPP consisting of photovoltaic cells (PV), battery energy storage systems (BESS), wind turbines (WT), and a conventional generator (CG) in the presence of varying loads. We numerically validate the proposed controller using both the learnt linearized dynamics and the actual nonlinear high-fidelity models of the FlexPower Plant. We also provide the practitioner with heuristic rules for tuning the proposed controller even in the absence of a plant model. Finally, in Section 7 we conclude and provide some potential directions for future research.

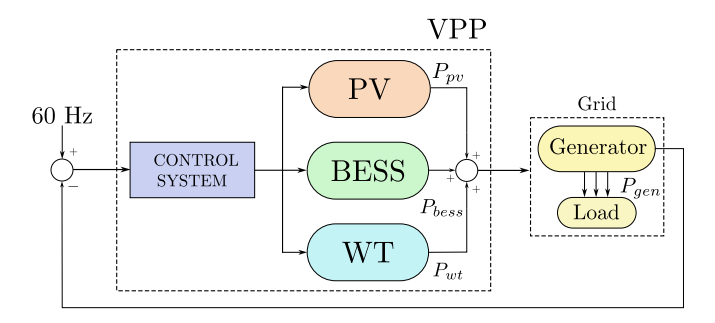


**Fig. 1.** Virtual power plant consisting of a grid (modeled by a synchronous machine and time-varying loads), DERs: PV, BESS, WT and a control system supplying active power reference signals for frequency regulation.

#### 3. Preliminaries

The proposed controller, termed Droop Reset Integral Control (DRIC), incorporates both continuous dynamics (i.e., integral action) and discrete time dynamics (i.e., integrator resets). To study this class of systems, we make use of the framework of hybrid dynamical systems [18]. For our purposes, it suffices to define a hybrid system as a dynamical system with state  $z \in \mathbb{R}^n$ , disturbance  $d \in \mathbb{R}^m$ , and the following dynamics:

$$z \in C$$
,  $\dot{z} = f(z, d)$ , (1a)

$$z \in \mathcal{D}, \qquad z^+ = g(z), \tag{1b}$$

where the system evolves, or "flows", in accordance with the differential equation with right hand side f when its state z is in the flow set C, and "jumps" according to (1b) when z is in the jump set D. In (1a), d can be seen as an external disturbance affecting the continuoustime dynamics. System (1) can be represented in compact form by the tuple  $\mathcal{H} = (C, f, D, g)$ . For the purpose of analysis, solutions to (1) are parameterized by a continuous-time index t, which increases continuously during flows (1a), and a discrete-time index j that increases by one during jumps (1b). Therefore, solutions to (1) are defined on hybrid time domains which are special subsets of the Cartesian product  $\mathbb{R}_{\geq 0} \times \mathbb{N}$ . For more details on the mathematical properties of hybrid systems we refer the reader to the Appendix. In this paper, we work with systems that satisfy the Hybrid Basic Conditions, see Definition 4 in Appendix.

We are interested in designing hybrid controllers that induce suitable closed-loop robust stability properties for the system. In particular, we are interested in achieving asymptotic bounds of the form

$$|z(t,j)| \le me^{-lt}|z(0,0)| + \gamma |d|_{\infty},$$
 (2)

for all  $(t,j) \in \text{dom}(z)$ , where  $m, \ell, \gamma > 0$ , and  $|d|_{\infty}$  is the standard infinite-norm of d, which is assumed to be bounded. Closed-loop systems that satisfy bounds of the form (2) for all initial conditions are said to be *finite gain exponentially input-to-state stable* (ISS) *from d to z* [19]. Our goal is to achieve this property in a class of VPPs controlled via DRIC.

#### 4. Problem formulation

We consider a VPP that consists of PV, BESS, and WT subsystems. These DERs are in turn connected to the grid which in our case, is modeled (macroscopically) by a conventional generator operating at 60 Hz and a variety of electrical loads that may be freely connected and disconnected in accordance with the demands imposed on the grid, see Fig. 1.

#### 4.1. Overall description of the VPP

The VPP under study is realized via a high-fidelity non-linear Simscape model designed by Sandia National Laboratories (termed the

FlexPower Plant [23]) wherein each DER is equipped with a control loop that enables the tracking of an active/reactive power reference within the ratings of the individual devices. As a consequence, we may view each DER as a "blackbox" power source, rendering the entirety of the VPP amenable to a frequency domain representation via model approximation. These representations may then be converted to a more suitable form for purposes of analysis using tools from hybrid control theory.

The PV and BESS components in the high-fidelity simulink-based model each have a DC-side voltage source, an averaged model of a voltage sourced inverter, a phase-locked loop, and individual current and voltage controllers modeled in the dq frame that provide droop and integral action coupled with feed-forward compensation. The current control loops generate input signals for the inverters. The wind turbine subsystem is modeled as a Type-4 WT, as detailed in [24], and it is also equipped with a turbine model with both pitch and torque control. The conventional generator (CG) consists of a synchronous machine equipped with an exciter and a governor that provides droop response. Lastly, in this work, all loads are modeled as three-phase parallel RLC branches. For a detailed description of the DER models, we refer the reader to [23,25]. Fig. 1 illustrates the scheme considered in the paper.

#### 4.2. Overall description of the control strategy

Within this setup, we solve the frequency regulation problem of driving the grid frequency to the nominal 60 Hz in the presence of a varying load profile by synergistically controlling the active power generated by the aforementioned DERs. In the proposed approach, we augment the PI (droop with integral action) controller with a *first order reset element* (FORE), which is a first-order dynamical system that incorporates a resetting integrator. As shown in the controls literature [13,19,26], this resetting action can be used to overcome some of the fundamental limitations, in terms of achievable transient performance (e.g., overshoot, settling time, etc.), of standard linear controllers. In particular, an integrator with resets is able to reduce the phase lag by 51.9° [13].

Based on this background, in this paper, we consider the following research questions: (1) How to design a robust frequency controller with integral and resetting action able to guarantee closed-loop stability when interconnected with the VPP? (2) How to guarantee that the proposed controller successfully rejects time-varying loads, recovering the steady-state operation of the plant with a minimal overshoot response and a reduced settling time? We shall answer question 1 in the affirmative via a theoretical guarantee in the next section and provide sufficient evidence for question 2 in Section 6 via comprehensive numerical experiments.

#### 5. Frequency regulation via droop reset integral control

In this section, we provide a detailed description of the model of the VPP and the resetting controller employed for the frequency regulation problem.

#### 5.1. Learnt voltage source inverter (VSI) dynamics

To account for the possibly non-linear dynamics of the individual DERs and obtain a suitable approximation of the system model, we impose a division of the range of available active power into a number of operating points. Each operating point is further divided into fringes which are meant to capture deviation from said point and are represented as percentages (see Fig. 2). Each fringe contributes training data in the form of a step response whose amplitude is equal to the fringe percentage times the operating point to which it belongs. This step signal/response (input/output) pair is fed to the system identification toolbox of the Matlab programming environment (see [27]) which, using the Instrumental Variables (IV) method (see [28]), returns a

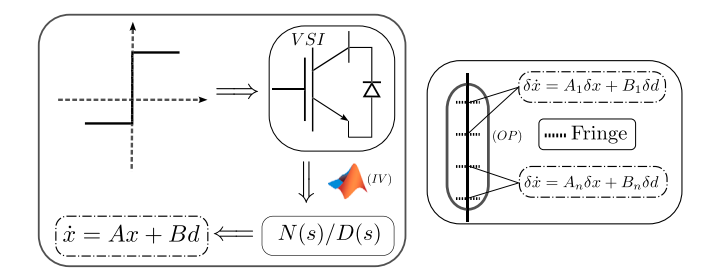


Fig. 2. The system identification process using instrumental variables (IV) (left). Division of operating point (OP) into fringes (right).

Table 1 Parameters for stability analysis via LMIs.

DER	A	В	С
PV	$\begin{bmatrix} -259.6460 & -2.9029 \cdot 10^4 \\ 1 & 0 \end{bmatrix}$	$\begin{bmatrix} 1 \\ 0 \end{bmatrix}$	$\begin{bmatrix} 1.3030 \\ 2.8979 \cdot 10^4 \end{bmatrix}^{T}$
BESS	$\begin{bmatrix} -258.5340 & -3.0408 \cdot 10^4 \\ 1 & 0 \end{bmatrix}$	$\begin{bmatrix} 1 \\ 0 \end{bmatrix}$	$\begin{bmatrix} 10.97 \\ 3.0392 \cdot 10^4 \end{bmatrix}^{T}$
WT	$\begin{bmatrix} -2.2250 & -7704 & -0.039 \\ 1 & 0 & 0 \\ 0 & 1 & 0 \end{bmatrix}$	$\begin{bmatrix} 1 \\ 0 \\ 0 \end{bmatrix}$	$\begin{bmatrix} -0.1111 \\ 0.3630 \\ 0.0496 \end{bmatrix}^{T}$
CG	-0.1429	1	0.1429

stable transfer function representation of the DER dynamics at the particular fringe with a pre-determined number of poles and zeros.

Using the training data from other fringes, the obtained transfer function is validated. Among the different models, the one that achieves best performance in terms of generalization is selected to represent the dynamics of the DERs near that operating point. Repeating this procedure on the remaining operating points gives us a holistic representation of the DER dynamics in the frequency domain under step responses. To obtain a single representation, we repeated the same generalization test on the set of learnt transfer functions.

#### 5.2. State-space representation of the VPP

Since all our analyses are most conveniently performed in the timedomain, we realize a state-space representation of the dynamics of the individual DERs. The PV and the BESS subsystems have states  $x_{pv}, x_{bess} \in \mathbb{R}^2$  respectively while the WT has state  $x_{wt} \in \mathbb{R}^3$ . The conventional generator is modeled as a synchronous machine via the swing equations as in [29] and has state  $x_{gen} \in \mathbb{R}$ . Loads are modeled as external disturbances d, and they enter the dynamics of the system only via the conventional generator as seen in Eq. (3d). The same equation also represents the cascade connection of the DERs and the CG. Based on this representation, we model the constituents of the VPPs as linear time-invariant systems given by:

PV: 
$$\begin{cases} \dot{x}_{pv} = A_{pv} x_{pv} + B_{pv} u \\ y_{pv} = C_{pv} x_{pv} \end{cases}$$
(3a)

BESS: 
$$\begin{cases} \dot{x}_{bess} = A_{bess} x_{bess} + B_{bess} u \\ y_{bess} = C_{bess} x_{bess} \end{cases}$$
(3b)

WT: 
$$\begin{cases} \dot{x}_{wt} = A_{wt} x_{wt} + B_{wt} u \\ y_{wt} = C_{wt} x_{wt} \end{cases}$$
(3c)

PV: 
$$\begin{cases} \dot{x}_{pv} &= A_{pv} x_{pv} + B_{pv} u \\ y_{pv} &= C_{pv} x_{pv} \end{cases}$$
(3a)
$$BESS: \begin{cases} \dot{x}_{bess} &= A_{bess} x_{bess} + B_{bess} u \\ y_{bess} &= C_{bess} x_{bess} \end{cases}$$
(3b)
$$WT: \begin{cases} \dot{x}_{wt} &= A_{wt} x_{wt} + B_{wt} u \\ y_{wt} &= C_{wt} x_{wt} \end{cases}$$
(3c)
$$Generator: \begin{cases} \dot{x}_{gen} &= a_{gen} x_{gen} + b_{gen} y_p + b_d d \\ y_{gen} &= c_{gen} x_{gen} \end{cases}$$
(3d)

Plant output: 
$$\{ y_p = y_{pv} + y_{bess} + y_{wt}.$$
 (3e)

External disturbances affecting the DERs could also be incorporated into our model by using additive vectors  $d_{pv}, d_{bess}, d_{wt}$  acting on the dynamics (3a)-(3c), similar to (3d). Table 1 depicts the values of the parameters we shall use for analysis in the following sections.

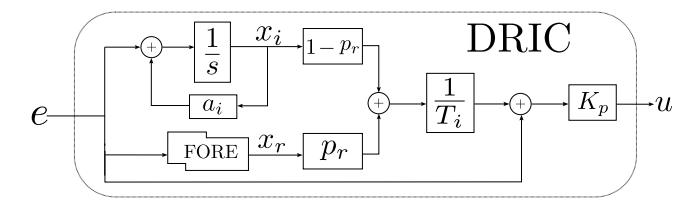


Fig. 3. Proposed control scheme: the standard droop with integral action augmented with a first order resetting integrator and weight  $p_r$  to ensure both steady-state and transient performance.

#### 5.3. Droop Reset Integral Controller (DRIC)

Our Droop Reset Integral Control (DRIC) system, depicted in Fig. 3, is a combination of the standard droop controller with integral action (PI), and a first-order reset element (FORE) which is a dynamical system with a first-order transfer function that additionally resets the integrator to zero whenever an algebraic relationship between its input and output is satisfied. The mathematical model of the DRIC has states  $x_i \in \mathbb{R}$  for the integrator and  $x_r \in \mathbb{R}$  for the FORE. The dynamics of the DRIC are described as follows:

If  $2ex_r \ge 0$  or  $\tau \le \rho$ :

$$\begin{pmatrix} \dot{x}_i \\ \dot{x}_r \end{pmatrix} = \begin{bmatrix} a_i & 0 \\ 0 & a_r \end{bmatrix} \begin{pmatrix} x_i \\ x_r \end{pmatrix} + \begin{pmatrix} 1 \\ 1 \end{pmatrix} e \tag{4a}$$

$$\dot{\tau} = 1. \tag{4b}$$

If  $2ex_r \le 0$  and  $\tau \ge \rho$ :

$$\begin{pmatrix} x_i^+ \\ x_r^+ \end{pmatrix} = \begin{bmatrix} 1 & 0 \\ 0 & 0 \end{bmatrix} \begin{pmatrix} x_i \\ x_r \end{pmatrix} \tag{5a}$$

$$\tau^+ = 0. \tag{5b}$$

The control signal acting on the VPP is then defined as:

$$u = \left[ \frac{(1 - p_r) \cdot k_p}{T_i} \quad \frac{p_r \cdot k_p}{T_i} \right] \begin{pmatrix} x_i \\ x_r \end{pmatrix} + k_p e. \tag{6}$$

where  $T_i, k_p > 0$  are tunable gains, and  $p_r \in [0, 1]$  is a tunable parameter used to weight the action of the FORE and the standard droop+integral control.

In the dynamics (4)–(5), the timer  $\tau$  is used to preclude the possibility of an infinite number of consecutive resets in a compact time interval, i.e., the so-called Zeno behavior. This type of temporal regularization is standard in the reset control literature, see for example [17]. The variable e, which usually models some form of tracking error, acts as the input to the controller. Based on this, the flow condition is satisfied when the input and the FORE state  $x_r$  have the same signs or when the timer has not yet crossed some threshold  $\rho$ . Similarly, the controller exhibits the discrete-time dynamics (5) when the input e and the state  $x_r$  have different signs and at least  $\rho$  units of time have passed since the last jump. During jumps, the state of the standard integrator is kept constant while the FORE state is reset to zero.

Finally, to illustrate the role of the parameter  $p_r \in [0, 1]$  in (6), we consider the two extreme cases. When  $p_r = 0$ , the DRIC degenerates into the standard droop controller with integral action realized by the proportional gain  $k_p$  and integral time constant  $T_i$ . On the other hand, when  $p_r = 1$  we realize a droop controller with resets. Both of these cases have their individual shortcomings: the standard PI controller suffers from fundamental phase limitations inherent to linear controllers, while in the other case the absence of an integral action may lead to non-zero steady-state errors. Therefore, the term  $p_r \in (0, 1)$ allows us to combine both control actions into the control signal u. Lastly, the negative terms  $a_i$  and  $a_r$  may be suitably tuned to achieve favorable transient performance (by shaping the overshoot response, see Fig. 4) and to simplify the stability analysis.

#### 5.4. Heuristic for dynamic control allocation

In addition to the DRIC dynamics elucidated by Eqs. (4)–(6), it is desirable in practical applications to include an additional mechanism that dynamically updates the reset ratio  $p_r$  to further improve the transient performance of the system. One such mechanism, commonly cited in the literature, uses the following update law for  $p_r$  [30, Ch. 5]:

$$p_r(t) = \bar{p}_r - t_D \frac{de_F}{dt},\tag{7}$$

where  $e_F$  is the tracking error passed through a low-pass filter so as to avoid the amplification of noise due to the derivative action. Intuitively, the update law (7) uses the predictive nature of the derivative term to increase the reset ratio while the error variable e is far away from its steady-state value. The parameter  $t_D$  is used to tune how strongly (weakly) the reset mechanism acts on the transient (steady-state) response.

#### 6. Results and simulations

In this section, we show that the proposed controller interconnected with the VPP achieves the stability property (2), and also improves the transient performance by reducing the overshoot and the settling time. We implement the control scheme in MATLAB/Simulink [31] and performed EMT (Electromagnetic Transient) simulations with a sampling time of  $10^{-5}$  s.

#### 6.1. Closed-loop model of the system

For the proposed controller, we can use the theoretical tools of [32] to study the stability properties of the closed-loop system. In particular, using the interconnection condition e = -y, our reset controller interconnected with the VPP model leads to the following closed-loop dynamical system:

$$\begin{aligned} \dot{\tau} &= 1 \\ \dot{x} &= Ax + B_d d \end{aligned} \right\}, & \text{if } x^\top M x \ge 0 \text{ or } \tau \le \rho, \\ \tau^+ &= 0 \\ x^+ &= A_r x, \end{aligned} \right\} & \text{if } x^\top M x \le 0 \text{ and } \tau \ge \rho,$$
 (8b)

$$\tau^{+} = 0$$

$$x^{+} = A_{r}x, \qquad \text{fif } x^{\top} M x \le 0 \text{ and } \tau \ge \rho, \tag{8b}$$

$$y = Cx (8c)$$

which has the form of (1). In particular,  $z = (\tau, x)$ , where  $x \in \mathbb{R}^{10}$ , and  $x = (x_{pv}, x_{bess}, x_{wt}, x_{gen}, x_i, x_r)$ , where the matrix A given by

$$A = \begin{bmatrix} A_p & B_p \\ -C_p \\ -C_p \end{bmatrix} & \Lambda_r \end{bmatrix}.$$

This matrix captures the plant dynamics

$$A_p = \begin{bmatrix} A_{pv} & O_{2\times 2} & O_{2\times 3} & -k_p B_{pv} c_{gen} \\ O_{2\times 2} & A_{bess} & O_{2\times 3} & -k_p B_{bess} c_{gen} \\ O_{3\times 2} & O_{3\times 2} & A_{wt} & -k_p B_{wt} c_{gen} \\ b_{gen} C_{pv} & b_{gen} C_{bess} & b_{gen} C_{wt} & a_{gen} \end{bmatrix},$$

the input interconnection

$$B_p = \begin{bmatrix} ((1-p_r)/T_i) \cdot k_p B_{pv} & (p_r/T_i) \cdot k_p B_{pv} \\ ((1-p_r)/T_i) \cdot k_p B_{bess} & (p_r/T_i) \cdot k_p B_{bess} \\ ((1-p_r)/T_i) \cdot k_p B_{wt} & (p_r/T_i) \cdot k_p B_{wt} \\ 0 & 0 \end{bmatrix},$$

the output interconnection

$$C_p = \begin{bmatrix} O_{7\times 1} & -c_{gen} \end{bmatrix},$$

and the continuous time dynamics of the DRIC in

$$\Lambda_r = \begin{bmatrix} a_i & 0 \\ 0 & a_r \end{bmatrix}.$$

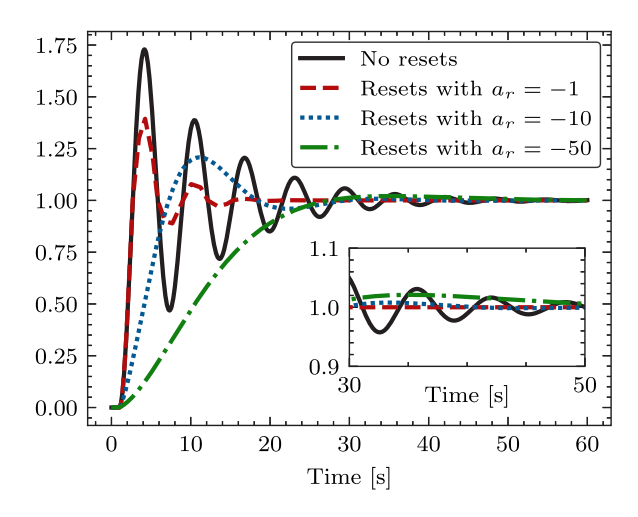


Fig. 4. Design imposed overshoot vs. settling time trade off on the plant P(s)(s+1)/s(s+0.2) via reset action from FORE.

Since the DRIC requires only the output of the conventional generator, the output matrix C takes the form

$$C = \begin{bmatrix} C_p & \mathcal{O}_{1 \times 2} \end{bmatrix}$$
.

For simplicity, we only consider disturbances acting on the conventional generator. As a result, the disturbance-to-state matrix has the

$$B_d = \begin{bmatrix} \mathbf{O}_{7 \times 1} & 1 & \mathbf{O}_{2 \times 1} \end{bmatrix}^\mathsf{T}$$
.

During jumps, we reset the state of the FORE and keep constant the remaining components of the state via the jump matrix

$$A_r = \begin{bmatrix} I_{9\times9} & \mathrm{O}_{9\times1} \\ \mathrm{O}_{1\times9} & \mathrm{O}_{1\times1} \end{bmatrix}.$$

Lastly, the sign-indefinite matrix M that describes the jump and flow sets is given by

$$M = \begin{bmatrix} \mathbf{O}_{9 \times 9} & -C_p^\top \\ -C_p & \mathbf{O}_{1 \times 1} \end{bmatrix}.$$

As shown in [26], in order to study the stability properties of systems of the form (8), it suffices to verify a family of Linear Matrix Inequalities (LMIs). The following proposition provides sufficient conditions for the stability and robustness of system (8).

Proposition 1. If the following two linear matrix inequalities (LMIs) on the variables  $P = P^{\top} > 0$ ,  $\tau_F$ ,  $\tau_R \ge 0$ ,  $\gamma > 0$  are feasible:

$$\begin{bmatrix} A^{\mathsf{T}}P + PA + \tau_F M & PB_d & C^{\mathsf{T}} \\ * & -\gamma I & 0 \\ * & * & -\gamma I \end{bmatrix} < 0, \tag{9a}$$

$$A_r^\top P A_r - P - \tau_R M \le 0, \tag{9b}$$

then, there exists  $\rho^* > 0$  such that for any fixed  $\rho \in (0, \rho^*)$ , the reset control system (6) interconnected with the plant is finite gain exponentially ISS from d to x.

We will use conditions (9) to numerically test the stability properties of the proposed DRIC controller interconnected with the VPP.

#### 6.2. Stability results for DRIC

To study the stability properties of the DRIC, we first consider the closed-loop system depicted in Fig. 1 consisting only of the PV and the BESS DERs. To verify stability, the LMIs (9) were implemented on the YALMIP optimization toolbox [33] using the parameter values supplied in Table 1 with the terms corresponding to the WT removed. In addition, the values of the gains of the integrators were set to  $a_i=-0.01$  and  $a_r=-100$ . MOSEK [34] reported that the LMIs were feasible with the following values:  $\tau_R=0.0223 \geq 0, \ \tau_F=2.196 \geq 0$  and  $\gamma=114.19>0$ . The matrix P was found to be symmetric and positive definite.

Next, the WT was added to the VPP and the finite-gain exponential stability of the resulting closed-loop system was checked using the LMI conditions (9) and the parameters from Table 1. The solver returned a feasible solution whose values were:  $\tau_R=0.0212 \geq 0$ ,  $\tau_F=2.1209 \geq 0$ ,  $\gamma=105.07>0$ . The matrix P was indeed symmetric and positive-definite.

The above results allow us to conclude that in both scenarios, the proposed DRIC renders the closed-loop system exponentially stable and ISS with respect to the disturbance d. In particular, bound (2) holds for the overall state x of the system. Moreover, by well-posedness of the hybrid model (1), we can also guarantee the existence of positive margins of robustness with respect to arbitrarily small additive disturbances acting on all the states and dynamics of the system [18, Thm. 7.21]. Such a robustness result is fundamental for practical applications where measurement noise and external perturbations are unavoidable.

#### 6.3. Numerical comparison between droop, DIC and DRIC

The prime efficacy of DRIC is in reducing the overshoot response generated by more traditional controllers like droop and PI. In practice, the "base" PI controller is usually first tuned using standard tools and then it is augmented with the proposed reset scheme. If the welltuned PI controller does not have a suitable transient response, one can deliberately detune it to achieve a faster response (at the cost of increased overshoot) and then use the reset scheme to remove or reduce the overshoot response [30]. Our first set of simulation results demonstrate this scenario on the learned models. First, we implement the VPP consisting of PV, BESS, WT and CG both using the learned VSI dynamics (see Section 5.1) and the high-fidelity Simscape model referenced in Section 4. Fig. 5 shows the response of the DRIC implemented on learned VSI dynamics to a time-varying load profile. It can be seen that upon the connection of a load, while the initial response of the DRIC is similar to the DIC, there is a considerable reduction in overshoot in the ensuing transient response. Indeed, there is a reduction of 0.35 Hz, 0.15 Hz, and 0.35 Hz respectively in the three load disturbances shown. Moreover, the settling time has also been drastically reduced from 15 s (DIC) to 3 s (DRIC) for all three load disturbances. This illustrates that the mere introduction of resets to a base linear controller is capable of significantly improving transient performance.

Next, we consider the scenario where a well-tuned PI controller is augmented with the reset scheme. We also compare standard linear controllers to our proposed scheme on the high-fidelity model. Fig. 6 compares standard linear controllers used for frequency regulation such as droop control and its integral variant (DIC) versus the proposed DRIC. As the inset shows, the droop controller suffers from non-zero steady-state error, eventually building up to a significant 2.5 Hz by the end of the run. This behavior is expected due to a lack of integral action. Clearly, subsequent load disturbances will result in instability as the droop controller is unable to keep the frequency within acceptable bounds. When augmented with integral action, the steady-state performance improves by 2.5 Hz, successfully regulating the frequency to the nominal 60 Hz well before the connection of subsequent loads. However, even a well-tuned DIC results in appreciable overshoot with the peak overshoot, ignoring the initial disturbance response, being 0.2 Hz, 0.1 Hz and just over 0.2 Hz respectively, for the three disturbances. In stark contrast, the DRIC retains the steady-state performance of the DIC (with an error of 0.0 Hz) and improves the transient performance. Once the initial disturbance is suppressed, the DRIC reduces overshoot by 0.2 Hz, 0.1 Hz, and 0.2 Hz respectively in the three load connections. Moreover, the nadir (lowest point of frequency) is reduced by 0.05 Hz,

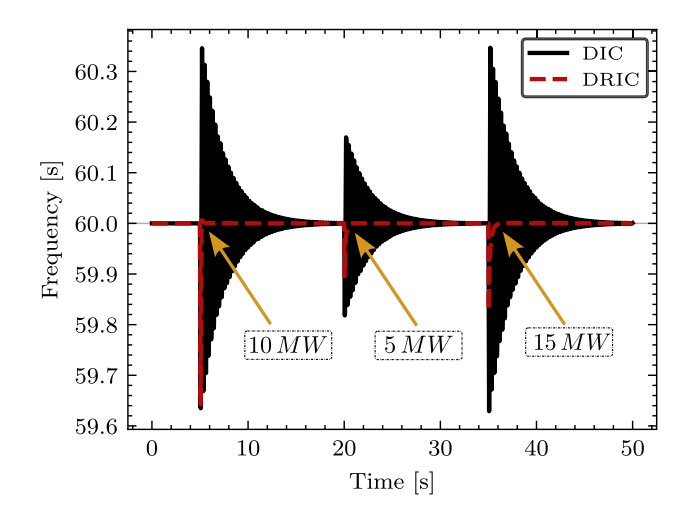
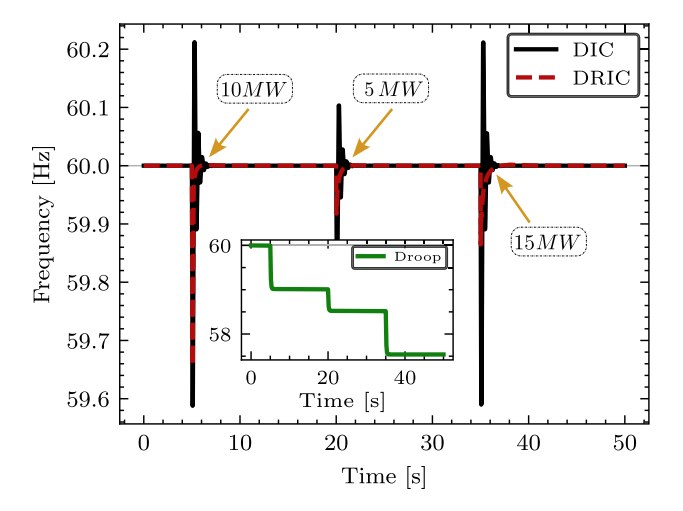


Fig. 5. DIC controller vs. DRIC on learned VSI dynamics.



 $\begin{tabular}{ll} Fig. 6. Well-tuned standard linear controllers vs. DRIC on VPP consisting of DERs: PV and BESS. \end{tabular}$ 

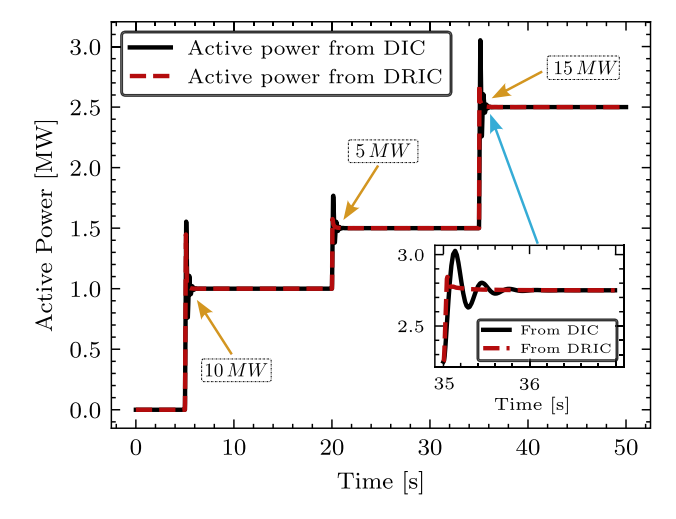


Fig. 7. Active power injection into CG from VPP consisting of PV and BESS in response to a time-varying load profile.

0.1 Hz, and 0.25 Hz respectively. The DRIC also results in a reduction of settling time by just over 1 s in the first load disturbance. In this scenario, the variable reset heuristic was incorporated to further

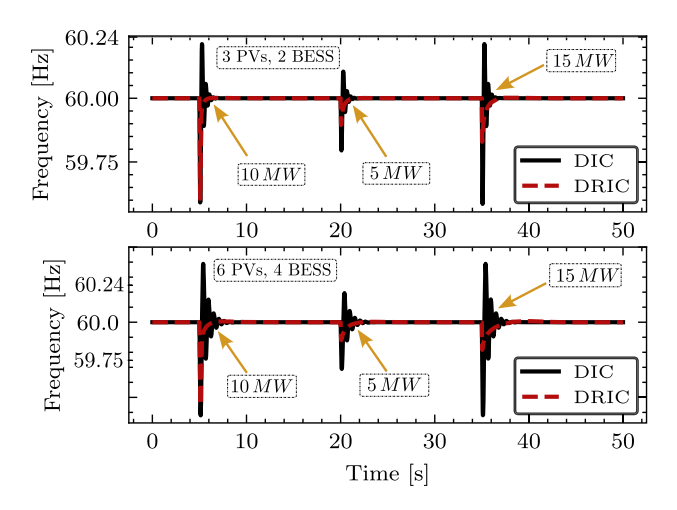


Fig. 8. DIC vs. DRIC on learnt VSI dynamics for VPPs consisting of 5 DERS (top) and 10 DERS (bottom).

improve the transient performance. This simulation shows that our proposed controller can outperform classic linear controllers by simply incorporating a resetting action into the integrator. It can be observed from the inset of Fig. 7 that the power injection obtained when implementing the DRIC exhibits less oscillations compared to the power injection obtained under a traditional DIC (droop + integral controller) algorithm. Indeed, the power injection from the DIC suffers from the classic oscillations induced by integral actions in proportional-integral controllers. This behavior is aligned with the one observed in the frequency response of the conventional generator in Fig. 6.

Fig. 8 shows a comparison of DIC vs. DRIC schemes for VPPs with a varying number of DERs in the VPP. In the first scenario (top), the VPP consists of three PV generators and two storage systems. It can be seen that DRIC outperforms the DIC in terms of overshoot response. Indeed, the reduction in overshoot is 0.4 Hz, 0.2 Hz, and 0.45 Hz respectively for the three load disturbances. In addition, we also see an improvement in settling time by 2 ss in the first load disturbance of 10MW. Of course, the DRIC retains the zero steady-state error of the DIC. It can also be seen that there is a reduction in the nadir with the most significant one being 0.4 Hz in the 15MW load disturbance response. In the second scenario (bottom), the VPP consists of 10 DERs, six of them being PV and four of them BESS. A similar response to the previous scenario is seen. However, this time, the overshoot generated by the DIC has increased. Still, the DRIC further reduces said overshoot by 0.2 Hz, 0.1 Hz, and 0.2 Hz respectively for the three load disturbances. The settling times remain relatively the same.

Next, we test the DRIC in the *high-fidelity* non-linear FlexPower Model. Fig. 9 shows a comparison between the results obtained with the proposed DRIC and the linear DIC (PI). In this case, after a initial transient, the frequency settles at 60 Hz until a disturbance of 10 MW is introduced at 10 s. The initial response matches that of the DIC controller but the disturbance is attenuated more effectively by DRIC. Moreover, DRIC achieves a steady-state condition at approximately 5 s before its linear counterpart. A similar response is evident in the disconnection of the load at 40 s. These numerical results on the high-fidelity model of the VPP showcase the potential improvements, in terms of transient performance, that can be achieved in frequency control by incorporating resetting actions. To the best of our knowledge, this is the first work that validates such approaches, analytically and numerically, for the frequency control of VPPs.

#### 6.4. Tuning guidelines for the system operator

In this section, we provide some heuristic tuning rules for implementing DRIC in practical applications without prior knowledge of the

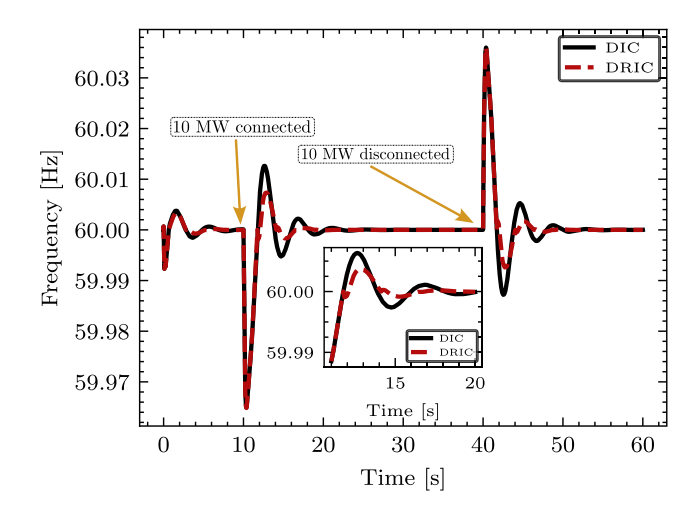


Fig. 9. Well-tuned DIC vs. DRIC on the high-fidelity model consisting of DERs: PV, BESS, and WT.

system model. We assume that the base linear controller, droop with integral action (DIC), in this case, has already been tuned via standard PI tuning algorithms, e.g., [22]. That is, values for  $k_p$  and  $T_i$  are known. Based on this, the following guidelines are in order:

- (a) Since the overarching goal is to have strong reset action over transients, and weak resets near steady-state, the parameter  $\bar{p}_r$  is typically tuned to have a small contribution when the derivative of the filtered error has small magnitude, i.e., near steady-state. A typical range for the nominal reset parameter is  $\bar{p}_r \in [0.05, 0.25]$  with smaller values used when weaker reset action is desired.
- (b) The parameter  $\rho$  affects how many jumps take place in a given interval of time. Higher values of  $\rho$  limit the number of possible resets while offering little safeguard against Zeno behavior. In the presence of a plant model, the value of  $\rho$  can be selected so as to satisfy the LMIs in Eq. (9). When no plant model is at hand, typical values of the parameter are  $\rho \in [0.1, 0.5]$ . This range was found to allow a sufficient number of jumps for the reset action to be effective, while avoiding Zeno behavior.
- (c) The parameter  $t_D$  affects the reset action influence when the response is away from the steady-state. Large values of  $t_D$  imply a higher variability in the resetting action away from the steady-state. Smaller values of  $t_d$  are used when a uniform resetting action is desired. As such the parameter  $t_D$  may be picked from a large range of [5, 200] depending on the application.
- (d) As mentioned earlier, in applications where the improvement in transient performance due to the resetting action is not substantial, the base controller may be detuned to increase its speed of response at the cost of increased overshoot. This overshoot can then be curtailed by tuning the FORE parameter a<sub>r</sub>. As is evident from Fig. 4, large negative values of a<sub>r</sub> suppress all of the overshoot at the cost of causing a delay in the settling time while smaller values trade off overshoot for reducing the settling time.

#### 7. Conclusions

We introduced a novel frequency control architecture for virtual power plants: Droop Reset Integral Control (DRIC). The proposed controller is designed to improve the transient performance of the system by reducing the overshoot and improving the settling time. To achieve these goals, the controller incorporates resetting integrators, which are triggered by suitable algebraic conditions on the inputs and outputs of the controller. While the area of reset control is fairly mature from the

theoretical standpoint, its applications in power systems had remained mostly unexplored. Yet, as shown in this paper, reset control is a technology that can be an effective alternative to improve transient performance in power systems that coordinate multiple DERs. Moreover, as also shown in this work, the stability properties of the system can be studied in linearized models using LMIs that can be numerically verified. Numerical validations were also performed on a high-fidelity non-linear model of a VPP (the FlexPower Plant) developed by the Sandia National Laboratories, as well as on models learned via model approximation from data generated by the VPP. It was observed that DRIC provides a substantial increase in transient performance.

Future research directions will focus on extending the proposed scheme to equip each DER with its own individual DRIC block. This distributed, asynchronous implementation could be suitable for large-scale systems that incorporate a large number of DERs. In this case, coordinating the resets of the controllers is imperative in order to achieve a suitable transient performance. Such decentralized coordination techniques are the subject of ongoing research. Other future research directions of interest include studying the performance of the proposed controller in networked VPPs in a power system with transmission lines, e.g., in an IEEE testing system. Additionally, the development of adaptive self-tuning mechanisms for the parameters of the controller is also an interesting future research direction.

#### CRediT authorship contribution statement

Vishal Shenoy: Conceptualization, Formal analysis, Investigation, Methodology, Validation, Writing – original draft, Writing – review & editing, Software. Paul Serna-Torre: Formal analysis, Investigation, Software, Writing – review & editing. David Schoenwald: Project administration, Supervision. Patricia Hidalgo-Gonzalez: Conceptualization, Project administration, Supervision, Validation, Writing – review & editing. Jorge I. Poveda: Conceptualization, Funding acquisition, Project administration, Supervision, Writing – original draft, Writing – review & editing.

#### Declaration of competing interest

The authors declare that they have no conflict of interest.

#### Data availability

Data will be made available on request.

#### Appendix. Hybrid dynamical systems

We present here some essential mathematical notions on hybrid dynamical systems of the form (1). Solutions to hybrid dynamical systems of the form (1) evolve on hybrid time domains which are special subsets of  $\mathbb{R}_{>0}\times\mathbb{N}.$ 

**Definition 1** (*Hybrid Time Domain*). A subset  $E \subset \mathbb{R}_{\geq 0} \times \mathbb{N}$  is a compact hybrid time domain if

$$E = \bigcup_{i=0}^{J-1} ([t_j, t_{j+1}, j])$$

for some finite sequence of times  $0=t_0\leq t_1\leq t_2\leq \cdots \leq t_J$ . It is a hybrid time domain if for all  $(T,J)\in E, E\cap ([0,T]\times \{0,1,\ldots,J\})$  is a compact hybrid time domain.

**Definition 2** (*Hybrid Arc*). A function  $z: E \to \mathbb{R}^n$  is a hybrid arc if E is a hybrid time domain and if for each  $j \in \mathbb{N}$ , the function  $t \mapsto z(t, j)$  is locally absolutely continuous on the interval  $I^j := \{t: (t, j) \in E\}$ .

A hybrid arc is a solution to a hybrid dynamical system (with inputs) if it satisfies two key properties which we mention below.

**Definition 3** (*Solution of a Hybrid Dynamical System*). A hybrid arc z is a solution to the hybrid dynamical system (C, f, D, g) given by (1) if  $z(0,0) \in \bar{C} \cup D$ , and

(S1) for all  $j \in \mathbb{N}$  such that  $I^j$  has non-empty interior

$$z(t,j) \in C$$
 for all  $t \in int I^j$ ,  
 $\dot{z}(t,j) = f(z(t,j),d(t))$  for all  $t \in I^j$ ;

(S2) for all  $(t, j) \in dom z$  such that  $(t, j + 1) \in dom z$ ,

$$z(t, j) \in D,$$
  
$$z(t, j + 1) = g(z(t, j)).$$

Trajectories of hybrid systems often converge to sets rather than equilibrium points (e.g., when periodic timers are part of the state z). Given a vector  $z \in \mathbb{R}^n$  and a compact set  $A \subset \mathbb{R}^n$ , the distance of z to A is denoted  $|z|_A$  and is defined by  $|z|_A := \min_{y \in A} |z-y|$ . To guarantee well-posedness, in this work we consider hybrid dynamical systems that satisfy certain regularity properties.

**Definition 4** (*Hybrid Basic Conditions*). The hybrid system (1) is said to satisfy the Basic Conditions if:

- The sets C and D are closed subsets of  $\mathbb{R}^n$ .
- The function  $f: \mathbb{R}^n \times \mathbb{R}^m \to \mathbb{R}^n$  is continuous.
- The function  $g: \mathbb{R}^n \to \mathbb{R}^n$  is continuous.

For a complete treatment of general hybrid systems, their solutions properties, stability notions and analysis tools, we refer the reader to [18].

#### References

- B. Tan, J. Zhao, M. Netto, V. Krishnan, V. Terzija, Y. Zhang, Power system inertia estimation: Review of methods and the impacts of converter-interfaced generations, Int. J. Electr. Power Energy Syst. 134 (2022) 107362.
- [2] C. Hodel, M. Beck, Overview of Ancillary Services, Swissgrid Ltd., Zurich, Switzerland. 2019.
- [3] S. Awerbuch, A. Preston, The Virtual Utility: Accounting, Technology & Competitive Aspects of the Emerging Industry, Vol. 26, Springer Science & Business Media, 2012.
- [4] D.E. Ochoa, F. Galarza-Jimenez, F. Wilches-Bernal, D. Schoenwald, J.I. Poveda, Control systems for low-inertia power grids: A survey on virtual power plants, IEEE Access (2023).
- [5] J.W. Simpson-Porco, F. Dörfler, F. Bullo, Synchronization and power sharing for droop-controlled inverters in islanded microgrids, Automatica 49 (9) (2013) 2603–2611.
- [6] T. Haines, F. Wilches-Bernal, R. Darbali-Zamora, M. Jiménez-Aparicio, Flexible control of synthetic inertia in co-located clusters of inverter-based resources, in: 2022 IEEE Power and Energy Conference at Illinois, PECI, IEEE, 2022, pp. 1–6.
- [7] E. Mallada, Idroop: A dynamic droop controller to decouple power grid's steadystate and dynamic performance, in: 2016 IEEE 55th Conference on Decision and Control, CDC, IEEE, 2016, pp. 4957–4964.
- [8] E. Tegling, M. Andreasson, J.W. Simpson-Porco, H. Sandberg, Improving performance of droop-controlled microgrids through distributed PI-control, in: 2016 American Control Conference, ACC, IEEE, 2016, pp. 2321–2327.
- [9] M. Minetti, A. Rosini, G.B. Denegri, A. Bonfiglio, R. Procopio, An advanced droop control strategy for reactive power assessment in islanded microgrids, IEEE Trans. Power Syst. 37 (4) (2022) 3014–3025.
- [10] M.M. Seron, J.H. Braslavsky, G.C. Goodwin, Fundamental Limitations in Filtering and Control, Springer Science & Business Media, 2012.
- [11] C. Dang, X. Tong, W. Song, Sliding-mode control in dq-frame for a three-phase grid-connected inverter with LCL-filter, J. Franklin Inst. 357 (15) (2020) 10159–10174.
- [12] T. Dragičević, Model predictive control of power converters for robust and fast operation of AC microgrids, IEEE Trans. Power Electron. 33 (7) (2017) 6304–6317.
- [13] J.C. Clegg, A nonlinear integrator for servomechanisms, Trans. Am. Inst. Electr. Eng. II 77 (1) (1958) 41–42.
- [14] O. Beker, C.V. Hollot, Y. Chait, Plant with integrator: an example of reset control overcoming limitations of linear feedback, IEEE Trans. Autom. Control 46 (11) (2001) 1797–1799.
- [15] O. Beker, C. Hollot, Y. Chait, H. Han, Fundamental properties of reset control systems, Automatica 40 (6) (2004) 905–915.

- [16] Y. Chait, C. Hollot, On Horowitz's contributions to reset control, Internat. J. Robust Nonlinear Control 12 (2002) 335–355.
- [17] L. Zaccarian, D. Nešić, A.R. Teel, First order reset elements and the Clegg integrator revisited, in: Proceedings of the 2005, American Control Conference, 2005, IEEE, 2005, pp. 563–568.
- [18] R. Goebel, R.G. Sanfelice, A.R. Teel, Hybrid Dynamical Systems: Modeling, Stability, and Robustness, Princeton, NJ, USA, 2012.
- [19] D. Nešić, A.R. Teel, L. Zaccarian, Stability and performance of SISO control systems with first-order reset elements, IEEE Trans. Autom. Control 56 (11) (2011) 2567–2582.
- [20] Z. Tu, B. Fan, J. Khazaei, W. Zhang, W. Liu, Optimal reset-control-based load frequency regulation in isolated microgrids, IEEE Trans. Sustain. Energy 13 (4) (2022) 2239–2249.
- [21] T. Banki, F. Faghihi, S. Soleymani, Frequency control of an island microgrid using reset control method in the presence of renewable sources and parametric uncertainty, Syst. Sci. Control Eng. 8 (1) (2020) 500–507.
- [22] A. Baños, A. Vidal, Definition and tuning of a PI + CI reset controller, in: 2007 European Control Conference, ECC, IEEE, 2007, pp. 4792–4798.
- [23] F. Wilches-Bernal, T. Haines, R. Darbali-Zamora, M. Jiménez-Aparicio, A resource aware droop control strategy for a PV, Wind, and Energy Storage Flexible Power (Flexpower) Plant, in: 2022 IEEE Kansas Power and Energy Conference, KPEC, IEEE, 2022, pp. 1–5.

- [24] K. Clark, N.W. Miller, J.J. Sanchez-Gasca, Modeling of GE wind turbinegenerators for grid studies, GE Energy 4 (2010) 0885–8950.
- [25] T. Haines, R. Darbali-Zamora, M. Jiménez-Aparicio, F. Wilches-Bernal, The impact of co-located clusters of inverter-based resources on a performance-based regulation market metric, in: 2022 North American Power Symposium, NAPS, IEEE, 2022, pp. 1–6.
- [26] D. Nešić, L. Zaccarian, A.R. Teel, Stability properties of reset systems, Automatica 44 (8) (2008) 2019–2026.
- [27] L. Ljung, R. Singh, Version 8 of the MATLAB system identification toolbox, IFAC Proc. Vol. 45 (16) (2012) 1826–1831.
- [28] P. Young, A. Jakeman, Refined instrumental variable methods of recursive time-series analysis part III. Extensions, Internat. J. Control 31 (4) (1980) 741–764
- [29] P. Kundur, Power System Stability and Control, McGraw-Hill Inc., 1994.
- [30] A. Baños, A. Barreiro, Reset Control Systems, Springer, 2012.
- [31] The MathWorks Inc., MATLAB Version: 9.14.0 (R2023a), The MathWorks Inc., Natick, Massachusetts, United States, 2023, [Online]. Available: https://www.mathworks.com.
- [32] L. Zaccarian, D. Nešić, A.R. Teel, Analytical and numerical Lyapunov functions for SISO linear control systems with first-order reset elements, Internat. J. Robust Nonlinear Control 21 (10) (2011) 1134–1158.
- [33] J. Lofberg, YALMIP: A toolbox for modeling and optimization in MATLAB, in: 2004 IEEE International Conference on Robotics and Automation (IEEE Cat. No. 04CH37508), IEEE, 2004, pp. 284–289.
- [34] E.D. Andersen, K.D. Andersen, The MOSEK interior point optimizer for linear programming: an implementation of the homogeneous algorithm, in: High Performance Optimization, Springer, 2000, pp. 197–232.